Biogeochemistry **23**: 169—196, 1993

Simulated effects of atmospheric sulfur deposition on nutrient cycling in a mixed deciduous forest

D. W. JOHNSON[1], W. T. SWANK[2] & J. M. VOSE[2]

[1] *Desert Research Institute, P.O. Box 60220, Reno, NV and Environmental and Resource Science, College of Agriculture, University of Nevada, Reno 89512, USA;* [2] *US Forest Service, Coweeta Hydrologic Laboratory, 999 Coweeta Lab Road, Otto, NC 28763, USA*

Received 27 May 1993; accepted 13 October 1993

Key words: aluminum, calcium, leaching, magnesium, potassium, soil, sulfur

Abstract. The effects of three S deposition scenarios — 50% reduction, no change, and 100% increase — on the cycles of N, P, S, K, Ca, and Mg in a mixed deciduous forest at Coweeta, North Carolina, were simulated using the Nutrient Cycling model (NuCM). The purpose of this exercise was to compare NuCM's output to observed soil and streamwater chemical changes and to explore NuCM's response to varying S deposition scenarios. Ecosystem S content and SO_4^{2-} leaching were controlled almost entirely by soil SO_4^{2-} adsorption in the simulations, which was in turn governed by the nature of the Langmuir isotherm set in the model. Both the simulations and the 20-year trends in streamwater SO_4^{2-} concentration suggest that the ecosystem is slowly becoming S saturated. The streamwater data suggest S saturation is occurring at a slower rate than indicated by the simulations, perhaps because of underestimation of organic S retention in the model. Both the simulations and field data indicated substantial declines in exchangeable bases in A and BA soil horizons, primarily due to vegetation uptake. The correspondence of model output with field data in this case was a result of after-the-fact calibration (i.e. setting weathering rates to very low values) rather than prediction, however. Model output suggests that soil exchangeable cation pools change rapidly, undergoing annual cycles and multi-decade fluctuations.

Varying S deposition had very little effect upon simulated vegetation growth, nutrient uptake, or N cycling. Varying S deposition strongly affected simulated Ca^{2+}, Mg^{2+}, K^+, and P leaching but caused little change in soil exchangeable pools of Ca^{2+} K^+, or P because soil exchangeable pools were large relative to fluxes. Soil exchangeable Mg^{2+} pools were reduced by high rates of S deposition but remained well above levels sufficient for tree growth. Although the total soil pools of exchangeable Ca^{2+} and K^+ were only slightly affected by S deposition, there was a redistribution of Ca^{2+} and K^+ from upper to lower horizons with increasing S deposition, causing increased base saturation in the deepest (BC) horizon. The 100% increased S deposition scenario caused increasing peaks in simulated Al^{3+} concentrations in A horizons after 25 years as a result of large seasonal pulses of SO_4^{2-} and lowered base saturation. Simulated soil solution Al^{3+} concentrations remained well below toxicity thresholds for selected tree species at the site.

Introduction

Nutrient cycling in forests has been modeled for over three decades, either conceptually (Rennie 1955; Cole et al. 1968; Duvigneaud & Denaeyer-DeSmet 1970; Curlin 1970; Miller et al. 1979) or mathematically (Shugart et al. 1976; Sollins et al. 1980; Pastor et al. 1987). Concerns over the effects of acidic deposition on surface waters has led to the formulation of several models emphasizing the interactions between soils, soil solution, and stream waters (Christopherson et al. 1982; Goldstein et al. 1984; Cosby et al. 1985; Reuss & Johnson 1986). Other models have addressed the effects of intensive forest harvesting on forest nutrient status and productivity and, consequently, emphasize nitrogen dynamics (Aber et al. 1980; Kimmins et al. 1984). As a part of the Integrated Forest Study (IFS), the Nutrient Cycling Model (NuCM) was developed to synthesize our current understanding of nutrient cycling in forests and to examine how they respond to changing sulfur and nitrogen atmospheric deposition rates (Johnson & Lindberg 1991; Liu et al. 1991a, b).

In this paper, NuCM is used to simulate the effects of various S deposition levels (current, 50% reduction, and 100% increase) on a mixed deciduous forest at Coweeta Hydrologic Laboratory, North Carolina. The purpose of this series of simulations was not to produce quantitative predictions of forest ecosystem response to S deposition, but to exercise the model, exploring the NuCM model's depiction of forest nutrient cycles at Coweeta to varying S deposition and determining how well simulated responses match actual data on soil and streamwater chemical changes through time.

Site and methods

The NuCM model

NuCM was developed as part of the Electric Power Research Institute's Integrated Forest Study primarily to examine the effects of atmospheric deposition on forest nutrient cycling (Liu et al. 1991, b; Johnson & Lindberg 1991). The NuCM model links the soil-solution chemical components of ILWAS model (Gherini et al. 1985) with traditional conceptual models of forest nutrient cycling on a stand level. NuCM differs from ILWAS in that it is oriented toward stand-level as opposed to watershed-level nutrient cycling. As a consequence, NuCM has a simpler hydrologic module and a more sophisticated vegetation cycling module. The available nutrients in soil strata and vegetation pools and the fluxes between them

are explicitly tracked and provided as model output. The model can be used to simulate forest response to atmospheric deposition and to various management practices (e.g. application of fertilizers). Factors included in the model allow the user to easily increase or decrease atmospheric deposition loads. A full description of NuCM is given by Liu et al. (1991a, b); only details pertinent to the current simulations are repeated here.

The forested ecosystem is represented as a series of vegetation and soil components. The model provides for both an overstory and understory, each of which can be divided into canopy, bole, and roots. Tree growth is a function of user-defined stand developmental stage and the availability of nutrients and moisture. Translocation of nutrients prior to senescence is also user-defined. The understory is simulated in a similar manner to the overstory, except that its 'incident precipitation' is the overstory's throughfall and its biomass nutrient concentrations are allowed to be different.

Using mass balance and transport formulations, the model tracks 16 solution-phase components including the major cations and anions (analytical totals), ANC (acid-neutralizing capacity), an organic acid analog, and total aluminum (Liu et al. 1991a, b). The concentrations of hydrogen ion, aluminum and carbonate species, and organic acid ligands and complexes are then calculated based upon the 16 components. The acid-base characteristics of the forest soil solution are computed by the model to properly account for the influence of hydrogen-ion concentration on cation exchange and mineral weathering.

The model routes precipitation through the canopy and soil layers, and simulates evapotranspiration, deep seepage, and lateral flow. The soil includes multiple layers (up to ten), and each layer can have different physical and chemical characteristics. The movement of water through the system is simulated using the continuity equation, Darcy's equation for permeable media flow, and Mannings equation for free surface flow. Percolation occurs between layers as a function of layer permeabilities and differences in moisture content. Lateral flow occurs in those layers with saturated moisture contents. The lower portion of a layer with average moisture level approaching saturation is also allowed to produce lateral flow. This is achieved using a linearization of Darcy's equation to account for variation in moisture content within that horizon (Liu et al. 1991a, b).

The model simulates processes which occur in the canopy, bole, and roots. The canopy intercepts wet and dry deposition and stores a fraction of the precipitation volume on the leaf surfaces, up to a user-defined interception storage capacity. The solution stored on the canopy undergoes chemical reaction with constituents on the leaf surface (e.g. foliar exudates), provides for direct nutrient uptake by the leaf, and is subject to concentration by evaporation. Dry deposition (gaseous, aerosol, and

particulate matter) is enhanced by the canopy in proportion to the leaf area index (LAI).

The nutrient pools associated with soil solution, the soil exchange complex, soil minerals, and soil organic matter are all tracked explicitly. The processes which govern interactions among these pools include decay, nitrification, anion adsorption, cation exchange and mineral weathering. Litter decay is represented as a series reaction with first order dependencies on the reactant concentrations and C/N ratios. The decay products include nutrients and organic matter — both solid (e.g. humus) and solution phase (e.g. organic acids). The nutrients produced enter the solution phase where they are available for uptake by vegetation or the exchange complex, and for transport from the forest floor by percolation and/or lateral flow.

The model simulates the noncompetitive adsorption of sulfate, phosphate, and organic acid. Sulfate adsorption can be simulated in NuCM using either linear or Langmuir adsorption isotherms. In these simulations, the Langmuir isotherm was used:

$$\text{Langmuir: } X = \frac{(X_{max})\,(b)\,(SO_4^{2-})}{1 + (b)\,(SO_4^{2-})} \tag{1}$$

where X_{max} = maximum sulfate that can be adsorbed on soil (a constant) and b = a constant. NuCM incorporates pH-dependent SO_4^{2-} adsorption into the Langmuir equation by setting $b = K\,(H^+)^2$, where K is an equilibrium constant for the equation,

$$K = \frac{X_{H_2SO_4}}{(Xs)\,(H^+)^2\,(SO_4^{2-})} \tag{2}$$

which describes the reaction:

$$X_S + 2(H^+) + SO_4^{2-} \rightarrow X_{H_2SO_4} \tag{3}$$

where $X_{H_2SO_4}$ = the number of sites onto which SO_4^{2-} is adsorbed = X in equation (1); X_s = unfilled adsorption sites and $X_{max} = X_{H_2SO_4} + X_S$. Phosphate adsorption in the model is represented by a linear isotherm.

Cation exchange is represented by the Gapon equation:

$$\frac{X_{M^{a+}}\,(M^{b+})^{1/b}}{X_{M^{b+}}\,(M^{a+})^{1/a}} = Q \tag{4}$$

where X = Exchange phase equivalent fraction; ( ) = Soil Solution

Activity (moles/L); M^{a+} = Cation of valence a; M^{b+} = Cation of valence b and Q = Selectivity Coefficient (constant).

We recognize the arguments presented by Sposito (1977) that the Gapon equation, as traditionally expressed, has no thermodynamic meaning because the activity of an exchange phase cannot be numerically related to the equivalent fraction. However, the Gapon equation was used in NuCM because Richter et al. (1991) found it to be robust (i.e. constant) with variations in ionic strength in a series of laboratory studies of Mg-Al exchange. Richter et al. (1991) attributed the relative stability of the Gapon equation largely to the fact that it takes concentrations to powers of 1 or less (1/2, 1/3) whereas the Vaneslow or Gaines-Thomas equation take concentrations to squares and cubes.

Mineral weathering reactions are normally slow and are described in the model using rate expressions with dependencies on the mass of mineral present and solution-phase hydrogen-ion concentration taken to a fractional power. Both mineral weathering rates and hydrogen ion dependencies are specified by the user, in contrast to the ILWAS model.

Model input is based on measurable parameters. All input is accomplished using a series of menus or automatic transfer of data from previously entered files. The model uses such data to compute selectivity coefficients for each soil layer simulated. Model output options include nutrient pool sizes, fluxes between components, the relative contribution or loss by process, and soil solution and adsorbed concentrations versus time. Long-term nutrient loss or accumulation can be tracked by following annual pool and flux charts. In these simulations, output data files were created and imported into EXCEL spreadsheets for the purposes of rearranging graphical presentations.

Calibration of NuCM

NuCM was calibrated using data from the Integrated Forest Study and from long-term records at Coweeta according to the procedures outlined in the User's Manual (Munson et al. 1992). This included input data files for physiographic, meteorological and atmospheric chemistry data; vegetation biomass, nutrient concentrations and growth data; soil physical data (horizon depths, bulk density, hydraulic conductivities, water retention characteristics, root distribution and uptake properties, and temperature); soil chemical data (primary minerals, mineral dissolution rates, mineral stoichiometries, and anion adsorption isotherm parameters); organic matter decay rates, and nitrification rates. Most of the input data was derived from Coweeta watershed 2, a reference watershed covered with a mature hardwood forest. Model parameters which were of no particular

consequence to our ecosystem and interests, or for which no site-specific data were available (such as organic acid adsorption, phosphate adsorption, snowmelt characteristics, fractions of leachable nutrients in litter, etc.) were left as in the original model formulation (Liu et al. 1991a, b). Multiple year simulations are conducted by repeating meteorological, precipitation, and air chemistry data inputs for the desired number of iterations.

As a consequence of NuCM's structure, calibrations were fairly accurate for some parameters which were largely a direct consequence of input data (i.e. vegetation and soil exchangeable contents) but less accurate for other parameters which were calculated less directly (e.g. atmospheric dry deposition, forest floor nutrient contents, leaching). In this context, there are two noteworthy items: (1) soil total nutrient contents were calculated from mineral composition and stoichiometry rather than directly from total concentrations, and (2) the first soil layer includes litter, and thus the properties of this layer were the average of litter and A horizon of the mineral soil. Soil chemical data requirements precluded the option of making layer 1 simply a litter layer. Calibration for parameters that were simulated, such as forest floor content, uptake, and leaching was done by trial and error. Table 1 summarizes actual (Swank et al. 1991) and first-year simulated values for ecosystem contents and fluxes. The largest deviations between actual and simulated contents were for S, which were in part a result of ecosystem changes from initial values even during the first year of simulation (vegetation S content) and in part a result of model structure (forest floor and soil extractable contents). Forest floor contents were simulated based upon litterfall and decomposition rates, which were adjusted to approximate actual N contents while minimizing deviations in the contents of other nutrients. NuCM does not differentiate among nutrients in terms of rate of release from forest floor. This resulted in lower simulated than actual contents in some cases (Ca, Mg, P) and higher simulated than actual in other cases (N, K, S).

During the process of calibration, soil hydraulic conductivity, the 'Evapotranspiration coefficient', and saturated hydraulic conductivities were used to match model output with known evapotranspiration rates, soil water flux and lateral flow values. Long-term stream discharge records at Coweeta greatly facilitated this phase of the calibration. Organic matter decay and nitrification rates were adjusted to obtain a compromise among acceptable rates of vegetation growth, forest floor change, and nitrate leaching. Because vegetation N increment was greater than atmospheric N inputs, soil organic matter decomposition rates were adjusted so that N mineralized from organic matter at a rate great enough to avoid growth decline due to N deficiency. An apparently unavoidable consequence of

Table 1. Actual (Swank et al. 1991) and year 2 simulated ecosystem contents and fluxes of N, P, S, K, Ca, and Mg.

	Vegetation		Forest Floor		Soil. Exch.		Soil. Total		Deposition		Uptake		Leaching	
	Act.	Sim.	Act.	Sim.	Act.	Sim.	Act.	Sim.	Act.	Sim.	Act.	Sim.	Act.	Sim.
	kmol ha^{-1}								kmol ha^{-1} yr^{-1}					
N	73.3	77.0	17.5	24.9	—	0.04	291	313	0.34	0.48	2.8	2.8	0.01	0.14
P	2.4	1.8	1.0	0.6	1.0	0.9	—	92	0.008	0.002	0.07	0.06	0.003	0.002
S	3.7	5.3	0.9	2.6	2.0	1.6	45	33	0.28	0.42	0.18	0.15	0.03	0.03
K	12.5	11.0	2.0	3.7	32.2	29.1	4261	4392	0.03	0.04	1.1	1.1	0.04	0.05
Ca	28.9	31.9	3.3	2.8	34.2	36.9	286	276	0.04	0.09	1.2	1.0	0.03	0.02
Mg	7.0	5.8	2.4	1.8	43.6	31.5	2809	3684	0.02	0.03	0.5	0.4	0.09	0.16

increasing soil organic matter decomposition and N mineralization was accelerated nitrate leaching. Consequently, simulated NO_3^- leaching was substantially greater than actual NO_3^- leaching. However, simulated net retention of N was still quite high, and NO_3^- was not the dominant anion in simulated soil solutions.

Simulated soil solution concentrations were calibrated to match actual values very closely at the beginning of the simulations (Month 0) except in the case of pH (Table 2). NuCM calculates pH from the Gapon exchange equation (equation 2), and ANC from pH and an input value for the partial pressure of CO_2 (pCO_2) in the soil. During the calibration, pCO_2 was manipulated so as to create ANC values which were initially close to actual values. The difference in pH values between the model and actual data may reflect model inaccuracy or CO_2 degassing from soil solutions prior to or during alkalinity titrations, which would cause a rise in pH from *in situ* levels. Thus, it is conceivable that 'actual' soil solution pH is closer to model output than the data in Table 2 indicate.

Table 2. Actual vs simulated soil solution concentrations for year 1.

Horizon	A		BA		BC	
	Actual	Simulated	Actual	Simulated	Actual	Simulated
	---------- $umol_c\ L^{-1}$ ----------					
ANC	14	13	16	15	11	8
Ca	20	20	9	9	4	4
Cl	28	25	17	28	21	22
K	29	29	13	13	5	5
Mg	62	62	63	63	28	28
Na	21	21	20	20	11	11
NH_4	0.54	0.50	0.53	0.50	0.38	0.50
NO_3	0.19	0.20	0.12	0.10	0.14	0.10
pH	5.69	4.70	5.80	4.32	5.78	4.50
H_2PO_4	0.42	0.40	1.98	2.00	0.22	0.22
SO_4	66	66	61	60	6	6
Al	2.15	2.15	0.31	0.31	0.29	0.29
pCO_2 (%)	0.18	1.66	0.16	4.67	0.12	1.54

In the following simulations, three alternative S deposition scenarios imposed: (1) No change (current inputs for 30 years), (2) 50% reduction, and (3) 100% increase. In all cases, simulations were run for 30 years.

Results

Increased sulfur deposition caused substantial increases in Ca^{2+}, K^+, Mg^{2+}, and SO_4^{2-} leaching over the 30-year simulation period (Table 3). Increased S deposition caused a reduction in P leaching because of increased phosphate adsorption due to lowered soil solution pH (shown later). Over the 30-year simulation, there were increases in vegetation N content (from both soil and atmospheric sources) and a small net ecosystem accumulation of N (approximately 10 kg ha^{-1}, or 0.4% of total ecosystem N) (Table 3 and Fig. 1). Increasing S deposition caused a slight increase in N leaching (Table 3), but negligible effects upon ecosystem N content because of the fact that leaching losses were very low relative to ecosystem contents (approximately 0.1%). In the cases of P, K, and Ca, there was a net redistribution from soil exchangeable/adsorbed pools to vegetation with little or no net change in total ecosystem content (Fig. 1). Increasing S deposition had negligible effects upon ecosystem P, K, and Ca contents despite the differences in leaching rate. (Changes in soil total pools of S, K, Ca, and Mg, not shown in Fig. 1, were negligible because weathering rates were set to very low values.) In the case of Mg, there were net losses from the exchangeable pool which caused appreciable (approximately 14%) net ecosystem losses. Increasing S deposition increased the net loss of exchangeable Mg appreciably (by about 14% from

Table 3. Simulated ecosystem fluxes under different S deposition scenarios.

	N	P	Ca	K	Mg	S
	kmol ha^{-1} 30 yr^{-1}					
Deposition						
50% Reduction	15.13	0.07	2.93	1.26	0.99	6.01
No change	15.13	0.07	2.93	1.26	0.99	12.01
100% Increase	15.13	0.07	2.93	1.26	0.99	24.02
Leaching						
50% Reduction	4.98	0.03	0.44	1.69	4.65	1.71
No change	5.21	0.03	0.60	1.85	5.30	3.23
100% Increase	5.48	0.02	1.37	2.24	7.16	7.51
Net balance						
50% Reduction	10.15	0.04	2.49	−0.43	−4.66	4.30
No change	9.92	0.04	2.33	−0.59	−5.31	8.78
100% Increase	9.65	0.05	1.56	−0.98	−7.17	16.51

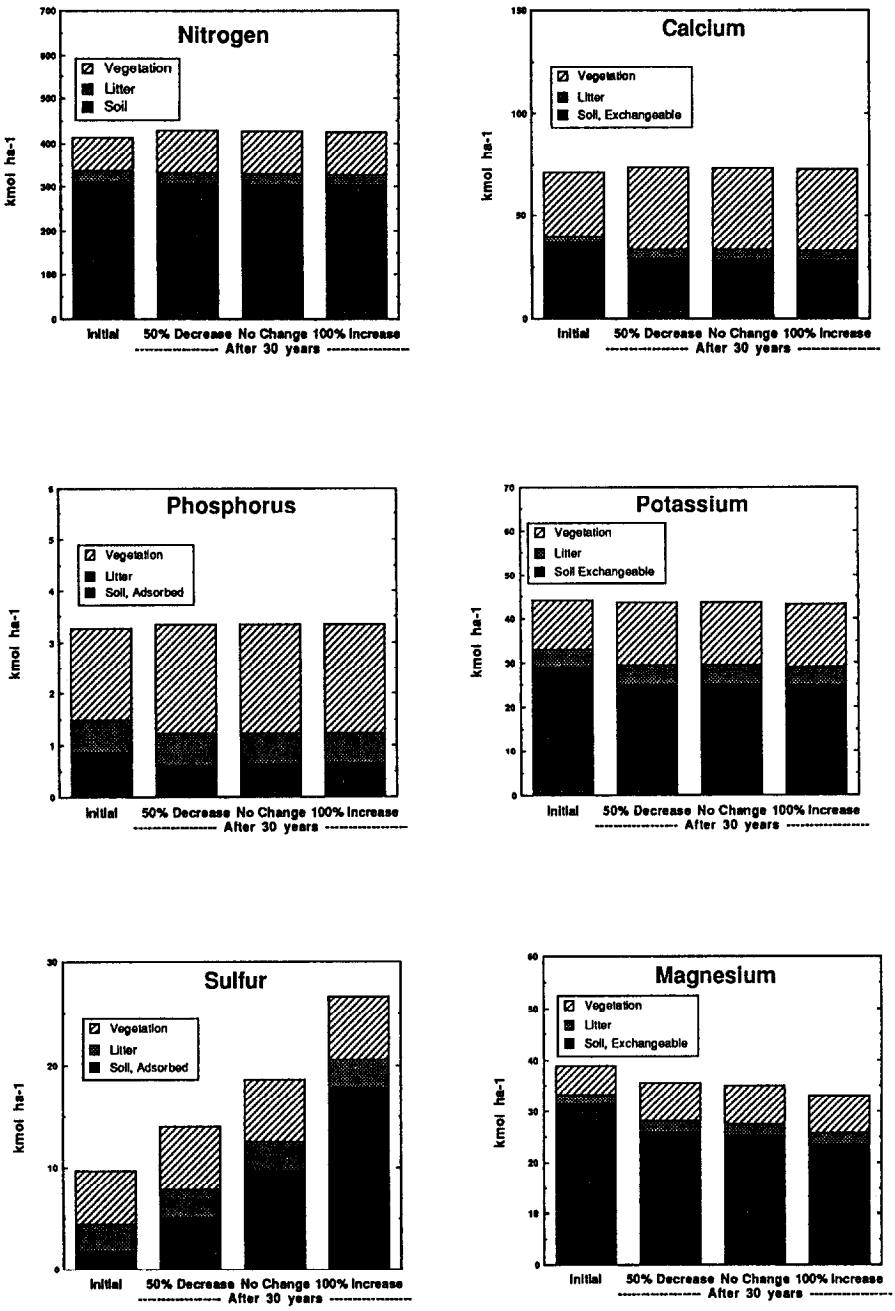

Fig. 1. Simulated ecosystem contents of N, P, S, K, Ca and Mg at Coweeta after 30 years under three S deposition scenarios.

the 50% reduction to the 100% increase scenario). In the case of S, there was a substantial net accumulation in the soil adsorbed pool and an overall increase in ecosystem content. Increasing S deposition caused substantial increases in soil adsorbed S pools (and, consequently, ecosystem S content) despite the large increases in S leaching with S deposition rate (Fig. 1 and Table 3).

Sulfate leaching rates increased steadily throughout the simulation and the differences due to S deposition became more pronounced with time (Fig. 2, top). In no case, however, was steady-state with respect to S input and output achieved within the 30-year simulation period (deposition was 0.208, 0.417, and 0.835 kmol ha^{-1} yr^{-1} in the 3 scenarios). In each S deposition scenario, soil adsorbed SO_4^{2-} continued to increase throughout the 30-year simulation (Fig. 2, middle). Despite the differences in S deposition and leaching, the percent ecosystem S retention with time were quite similar (Fig. 2 bottom). Experimentation with other S scenarios showed that steady-state was achieved immediately and maintained over the 30-year simulation period when current S inputs were reduced by 90%.

Calcium, K^+ and Mg^{2+} leaching were driven primarily by SO_4^{2-}, and thus the differences due to S deposition became increasingly pronounced with time (Fig. 3). Calcium, K^+ and Mg^{2+} leaching deviated from the patterns in SO_4^{2-} leaching to the extent that BC horizon exchangeable pools changed. In the case of Ca^{2+} there were declines in exchangeable concentrations over the 30 year simulation under the No Change scenario (especially in BA horizon) due to a combination of uptake and leaching (Fig. 4). Increasing S deposition slightly enhanced the decline in A horizon exchangeable Ca^{2+}, but reduced the decline in BA horizon exchangeable Ca^{2+} and increased BC horizon exchangeable Ca^{2+}. Thus, there was a net redistribution of exchangeable Ca^{2+} from the A to the BA and BC horizons with increased S deposition and SO_4^{2-} leaching. In the case of K^+, there were declines in exchangeable concentrations in the A and BA horizons which were enhanced by increasing S deposition, but there was evidence of redistribution as the BC horizon exchangeable K^+ increased slightly with increasing S deposition (Fig. 5). In the case of Mg^{2+}, the reductions in exchangeable concentrations in the A and BA horizons were enhanced by increasing S deposition, but there was no evidence of redistribution (i.e. S deposition effects were negligible in the BC horizon) (Fig. 6). Simulated base saturation declined in the A and BA horizons over the 30-year simulation, and the declines were enhanced by increasing S deposition (Fig. 7). The redistribution effect was evident in the BC horizon, where increasing S deposition accentuated the initial increases

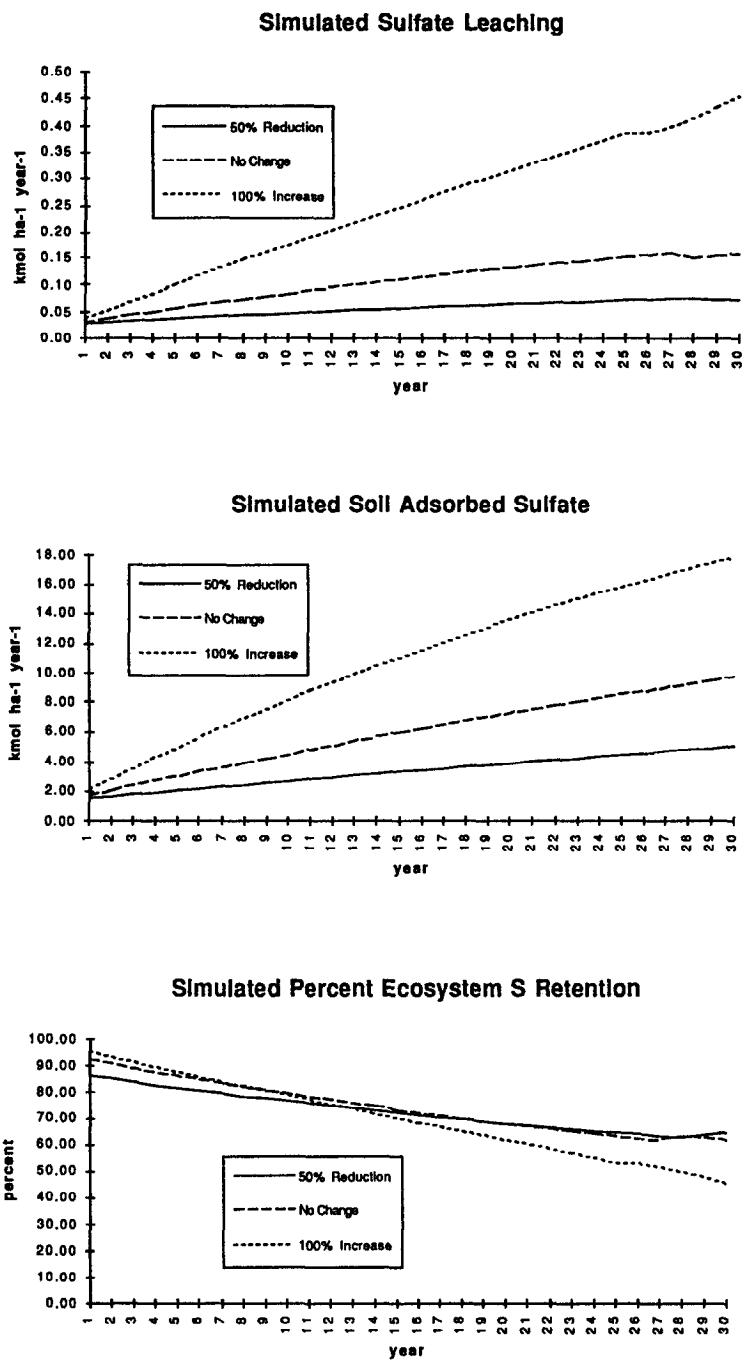

Fig. 2. Simulated sulfate leaching (top), soil adsorbed sulfate (middle), and percent ecosystem S retention (bottom) under three S deposition scenarios at Coweeta.

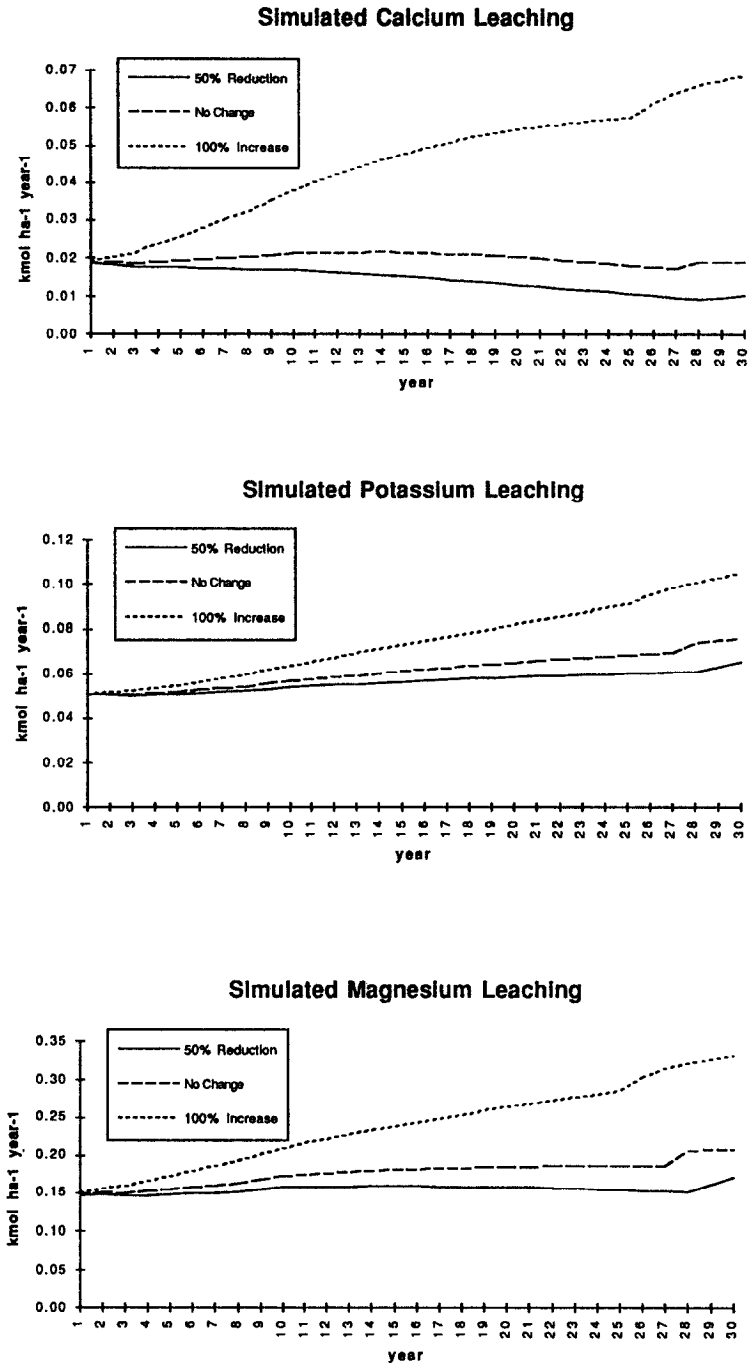

Fig. 3. Simulated leaching of Ca (top), K (middle), and Mg (bottom) under three S deposition scenarios at Coweeta.

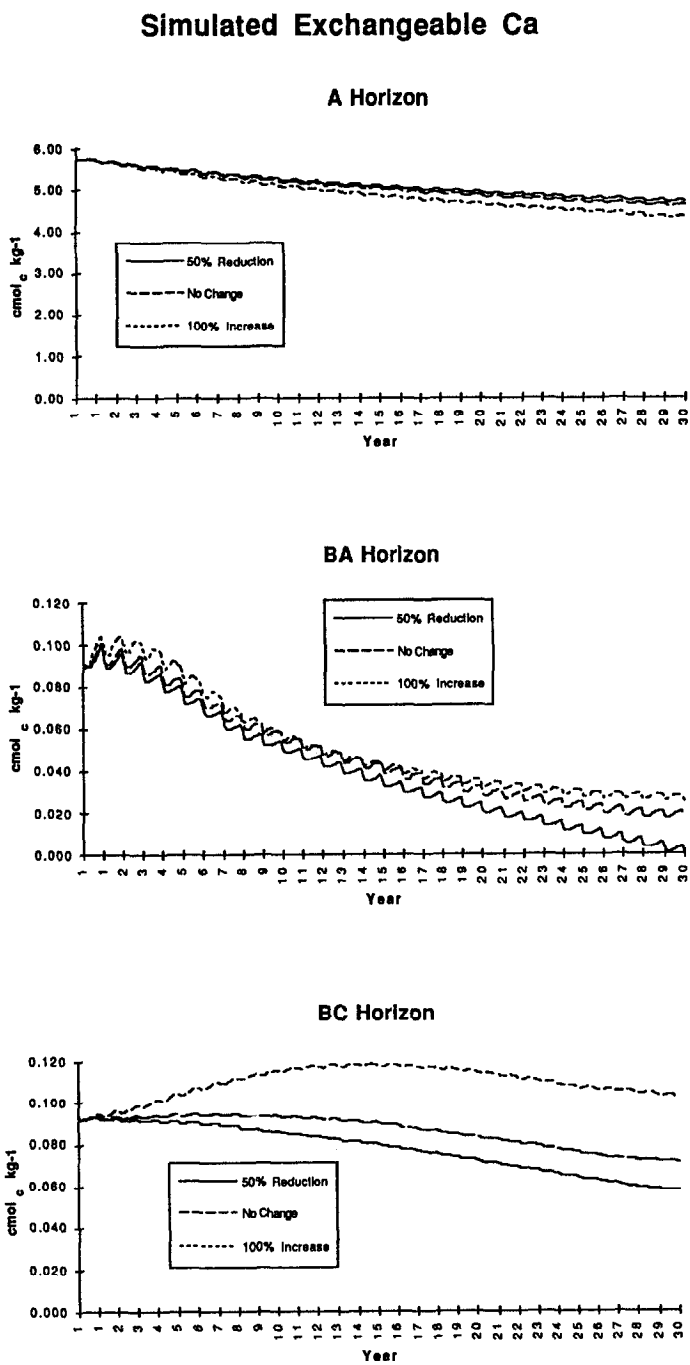

Fig. 4. Simulated changes in exchangeable Ca^{2+} at Coweeta under three S deposition scenarios.

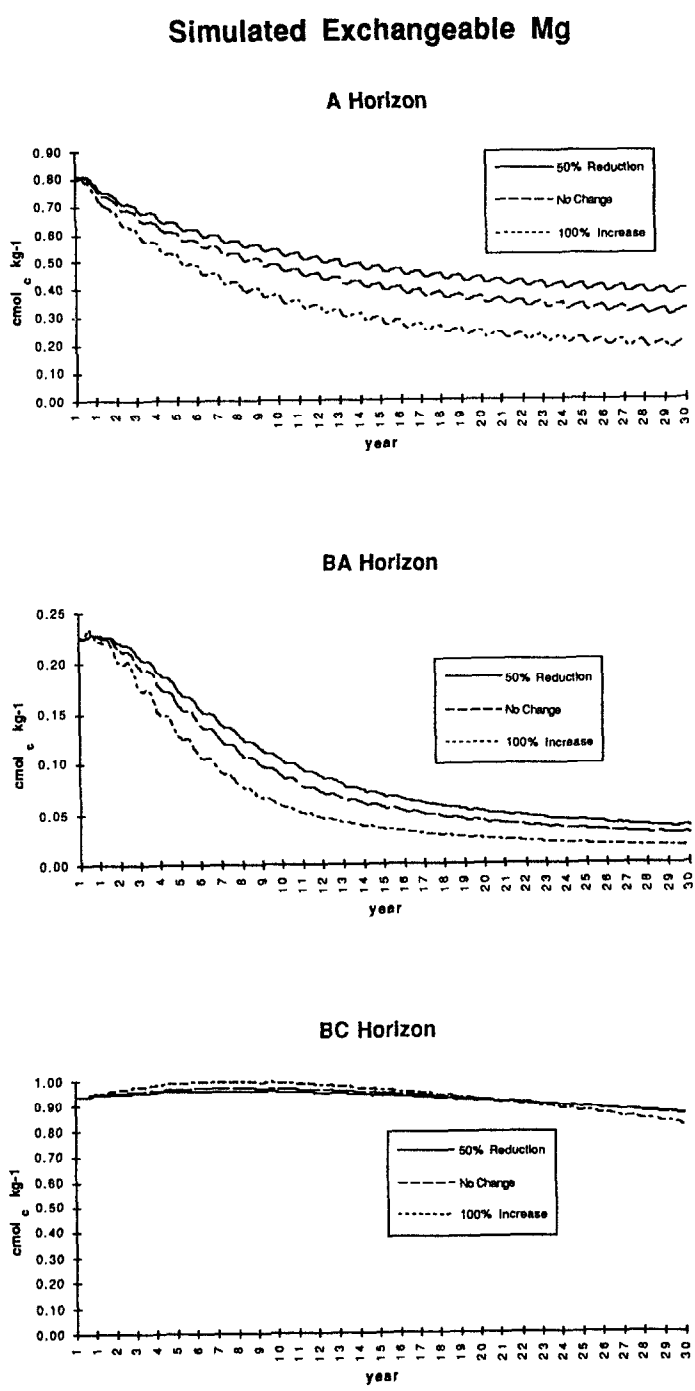

Fig. 5. Simulated changes in exchangeable Mg^{2+} at Coweeta under three S deposition scenarios.

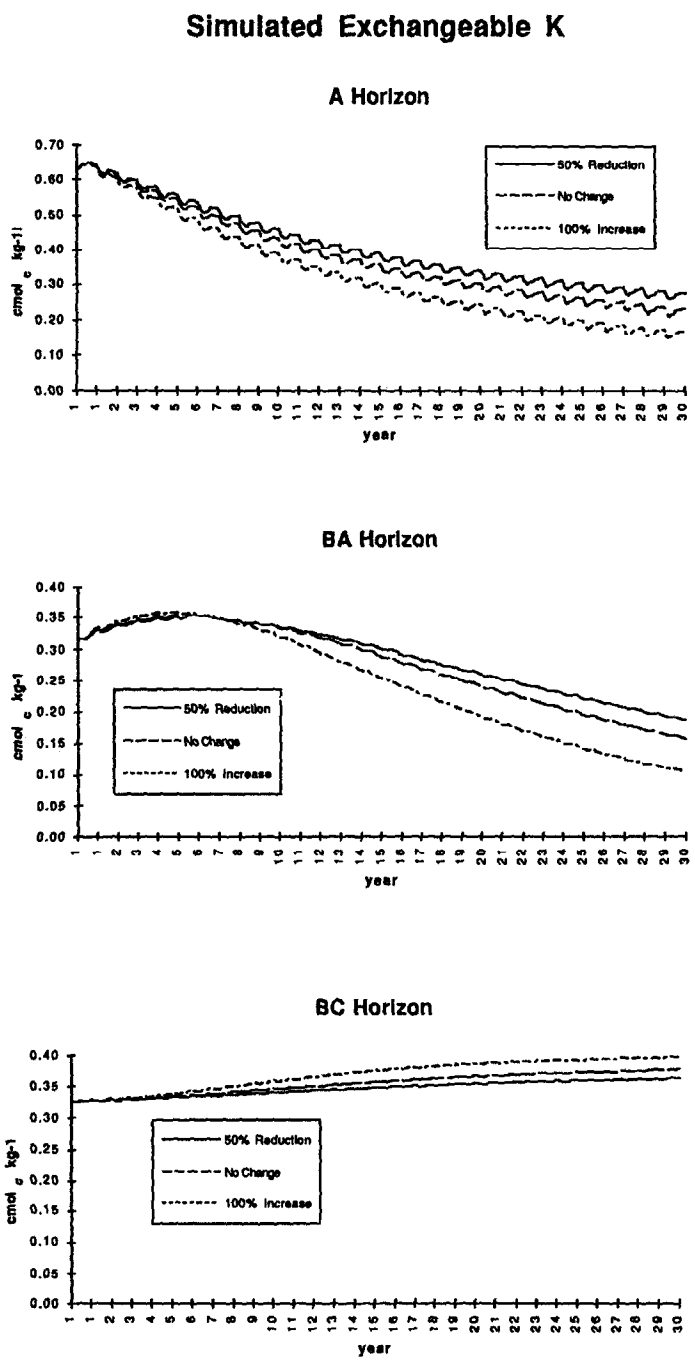

Fig. 6. Simulated changes in exchangeable K^+ at Coweeta under three S deposition scenarios.

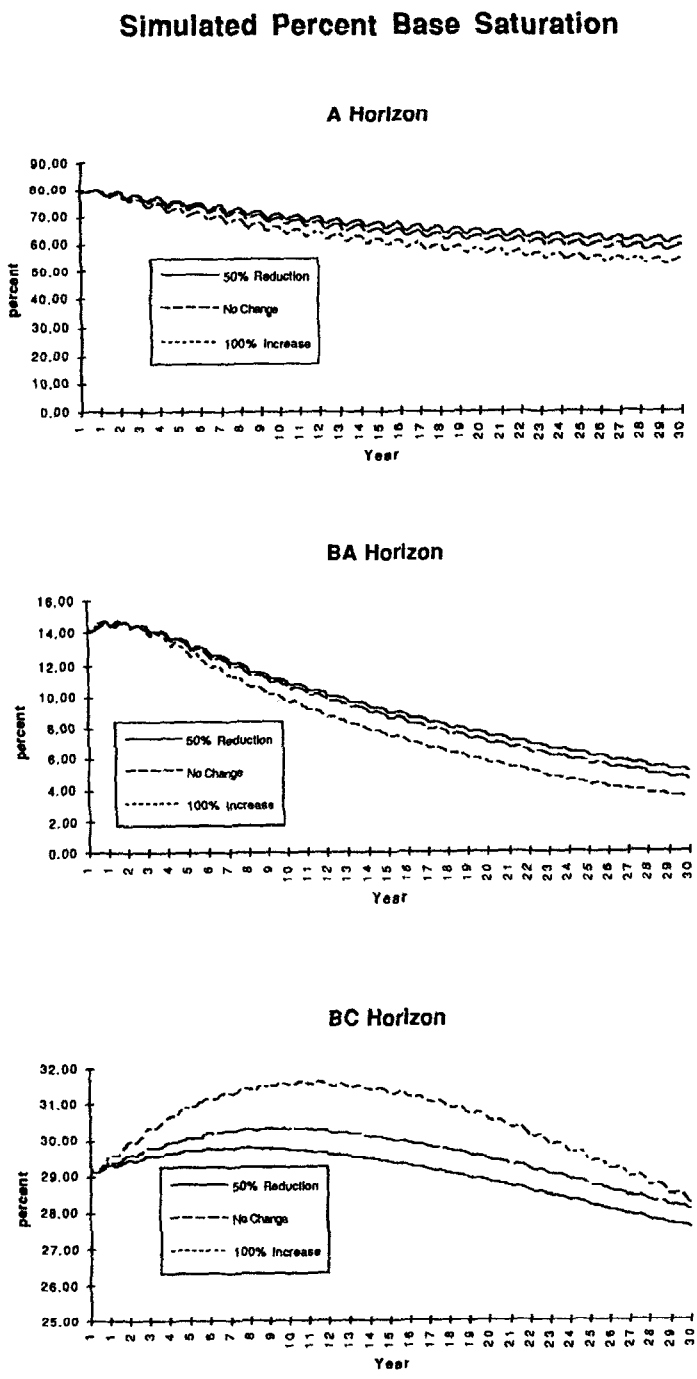

Fig. 7. Simulated changes in percent base saturation at Coweeta under three S deposition scenarios.

from years 1 to 12 and resulted in greater base saturation which lasted until the end of the 30-year simulation.

The changes in base saturation, coupled with changes in soil solution SO_4^{2-} concentration, caused changes in soil solution pH, ANC and Al^{3+}. Due to soil solution concentrating effects during summer droughts, summertime soil solution SO_4^{2-} concentrations under the 100% increase scenario peaked at over 1000 and 500 $umol_c\ L^{-1}$ in the A and BA horizons, respectively (Fig. 8). As a result, A and BA horizon soil solution pH began to show seasonal decreases to below 4.0 and soil solution Al^{3+} levels rose from less than 1 to 35 and 170 $umol_c\ L^{-1}$ under the 100% increase scenario (Figs. 9 and 10). Sulfate breakthrough and soil solution SO_4^{2-} peak values leveled off substantially after 10 years in the A and BA horizons (Fig. 8), but peak soil solution Al^{3+} values continued to increase after 10 years because of continuing decreases in base saturation (Fig. 7). In the BC horizon, high soil SO_4^{2-} adsorption capacity substantially buffered the summertime soil solution SO_4^{2-}, pH, and Al^{3+} fluctuations in the early years of the simulation. Late in the simulation, however, (after 27 years), the soil system reached higher points on the SO_4^{2-} adsorption isotherm (Fig. 11; see discussion below) where buffering of soil solution SO_4^{2-} was less intense (the slope of the isotherm was less) allowing soil solution SO_4^{2-} and, consequently, Al^{3+} to experience substantially greater seasonal variations (Figs. 8 and 10). Soil solution Al^{3+} concentrations remained quite low ($< 3\ umol_c\ L^{-1}$) in the BC horizon, however.

Discussion

Johnson & Reuss (1984) noted that, 'because sulfate adsorption is concentration-dependent, the time required to achieve equilibrium may not be materially shortened by an increase in the impact dosage'. The results of these simulations would tend to support this contention (i.e. Fig. 2, bottom). However, the time required to achieve steady-state (equilibrium) is not entirely independent of the impact dosage, in that the latter may affect the amount of soil adsorbed sulfate. Soil solution SO_4^{2-} concentration becomes increasingly responsive to changes in soil adsorbed sulfate as the latter increases, as can be seen from the slope (first derivative) of the adsorption isopleth. Solving the Langmuir equation (equation 1) for (SO_4^{2-}) and taking the first derivative yields:

$$\frac{dSO_4^{2-}}{dX} = \frac{X_{max}}{b(X_{max} - X)^2} \qquad (5)$$

for $X < X_{max}$.

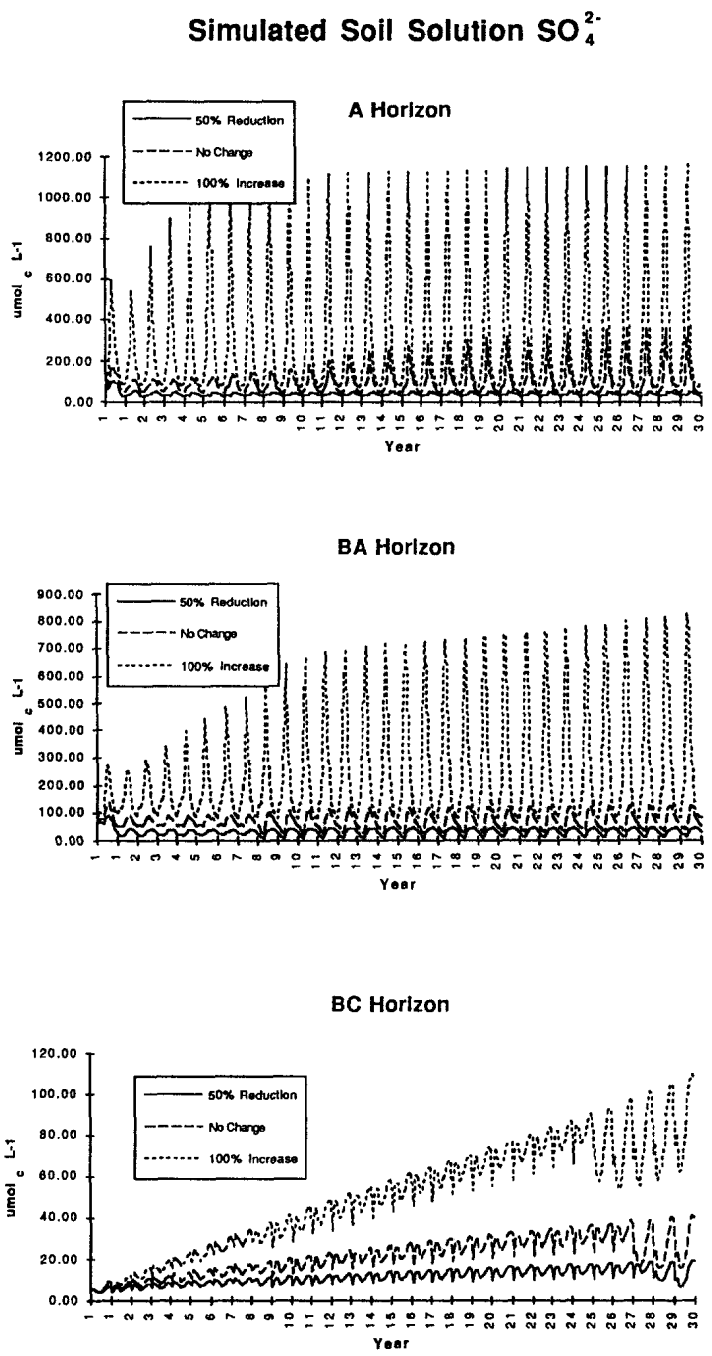

Fig. 8. Simulated soil solution SO_4^{2-} concentrations under three S deposition scenarios at Coweeta.

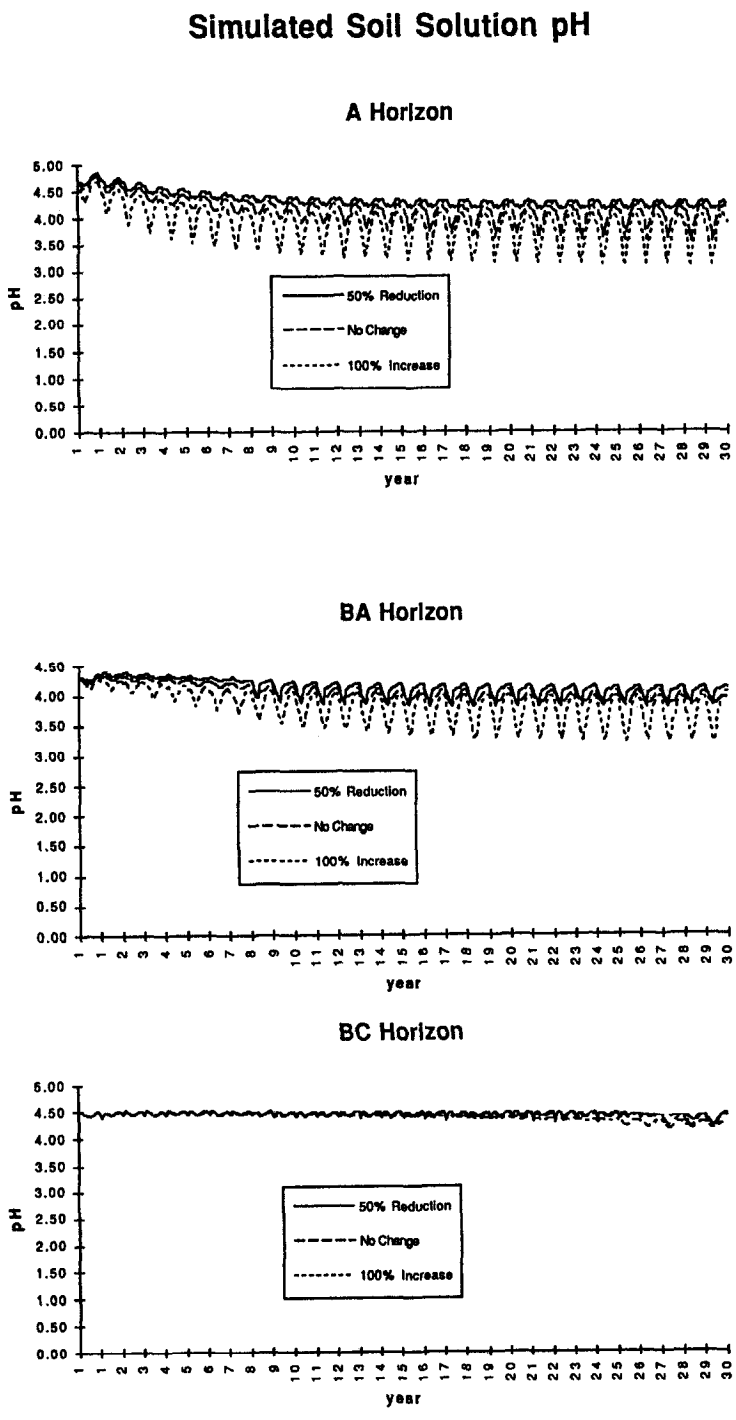

Fig. 9. Simulated soil solution pH under three S deposition scenarios at Coweeta.

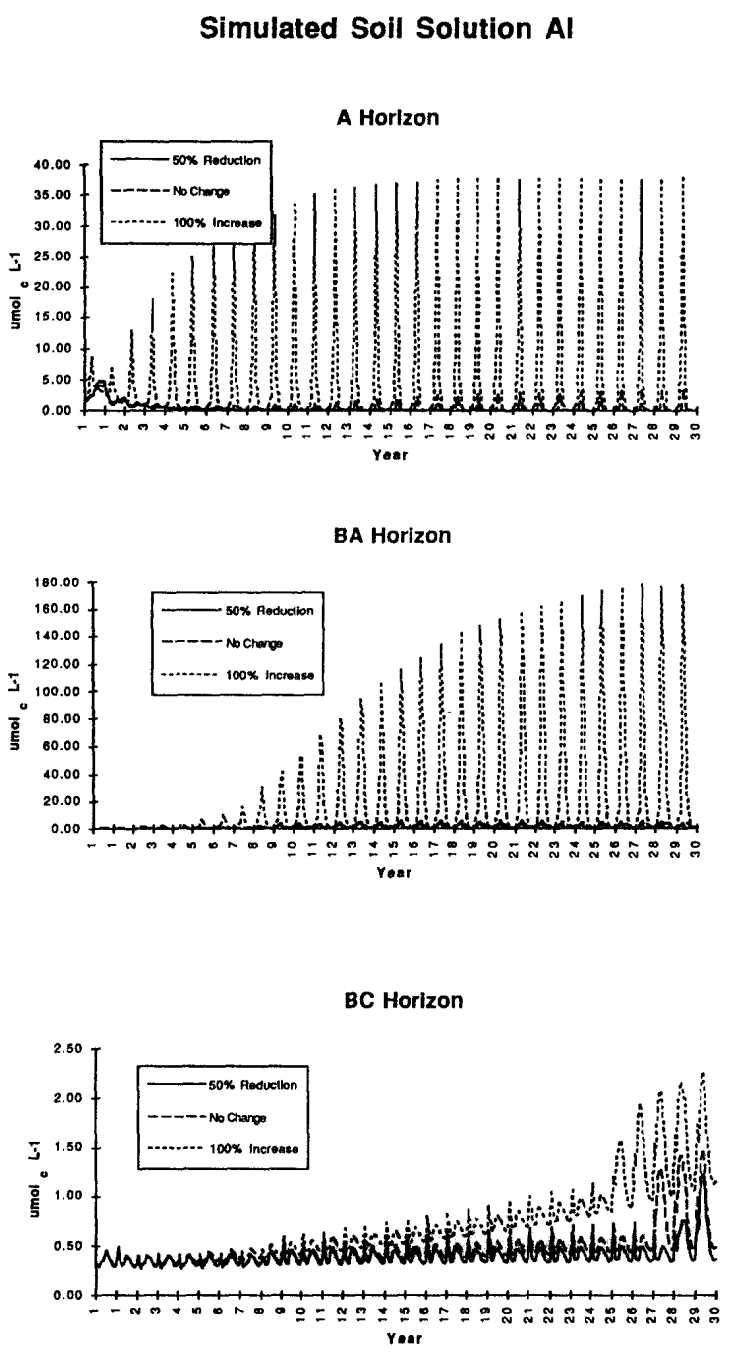

Fig. 10. Simulated soil solution Al^{3+} concentrations under three S deposition scenarios at Coweeta.

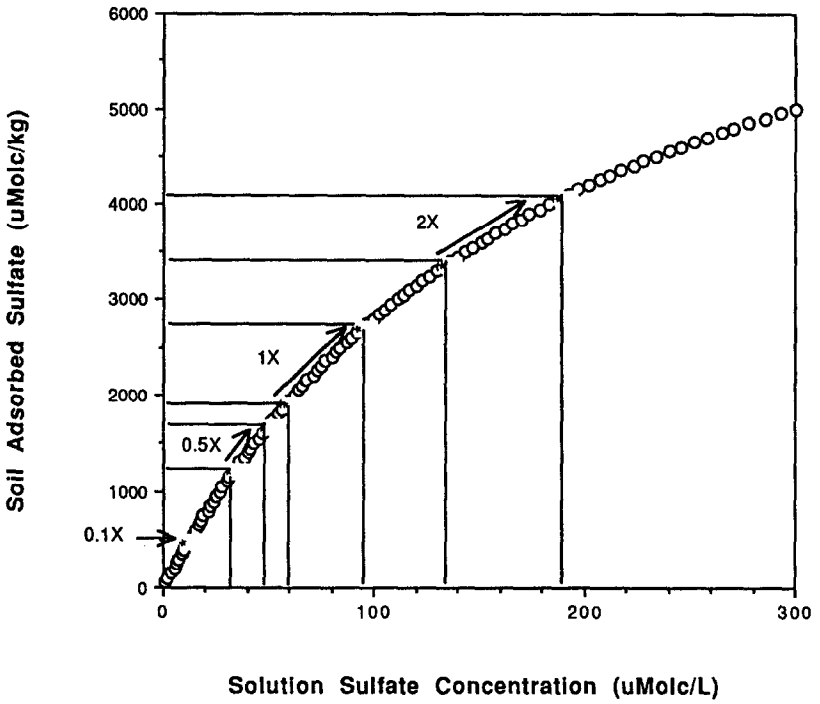

Fig. 11. The Langmuir soil sulfate adsorption isotherm used in B horizon simulations at Coweeta. Arrows show the ending points of the soil sulfate system under the three S deposition scenarios (beginning of arrows) and steady-state (end of arrows).

Thus, the responsiveness of soil solution SO_4^{2-} to increases in soil adsorbed sulfate (and, therefore to increase sulfate inputs to the system) increases as the soil becomes 'saturated' with SO_4^{2-}; i.e. as X increases and approaches X_{max}, $d(SO_4^{2-})/dX$ increases. This can be seen in Fig. 11, where the ending point of each 30-year simulation (beginning of each arrow) and the steady-state values (end of each arrow) for soil adsorbed sulfate versus solution SO_4^{2-} concentration are plotted on the Langmuir isotherm used in the simulations. After 30 years, the soils under the three deposition scenarios were on portions of the isotherm with significantly differing slopes, reflecting different responsiveness, or, conversely, buffering capacity, for a given SO_4^{2-} input. Thus, the responsiveness of soil solution SO_4^{2-} to a given input of SO_4^{2-} in year 30 is 100% Increase > No Change > 50% Decrease (and the reverse order applies to degree of SO_4^{2-} retention).

The situation with respect to soil SO_4^{2-} adsorption and SO_4^{2-} leaching becomes considerably more complicated when pH changes are substantial, causing variations in pH-dependent soil SO_4^{2-} adsorption. In such a situation, it is very unlikely that the simple analyses given above would suffice to explain SO_4^{2-} behavior in the soil system, and a simulation modeling approach may add substantial insight into system behavior. In these simulations, however, soil solution pH changes in the BC horizon, where over 90% of the total soil adsorbed SO_4^{2-} pool lay, were slight (Fig. 9, bottom).

Long-term trends in stream SO_4^{2-} concentration at Coweeta corroborate NuCM's predictions of increasing soil SO_4^{2-} saturation. Figure 12 shows a comparison of the regression equation describing the observed increase in stream SO_4^{2-} from 1970 to 1990 in watershed 18, a reference watershed (Swank & Waide 1988), with simulated average annual BC soil solution SO_4^{2-} concentrations for the No Change S deposition scenario for the first 20 years of the simulation. Streamwater SO_4^{2-} concentrations increased steadily, but at a slower rate than simulated BC horizon SO_4^{2-} concentration from years 1 to 20. There are several possible reasons for this difference. One possibility is that soil SO_4^{2-} adsorption in the field is greater than determined in the laboratory. (Recall that the values used to parameterize the Langmuir equation in this simulation were obtained from

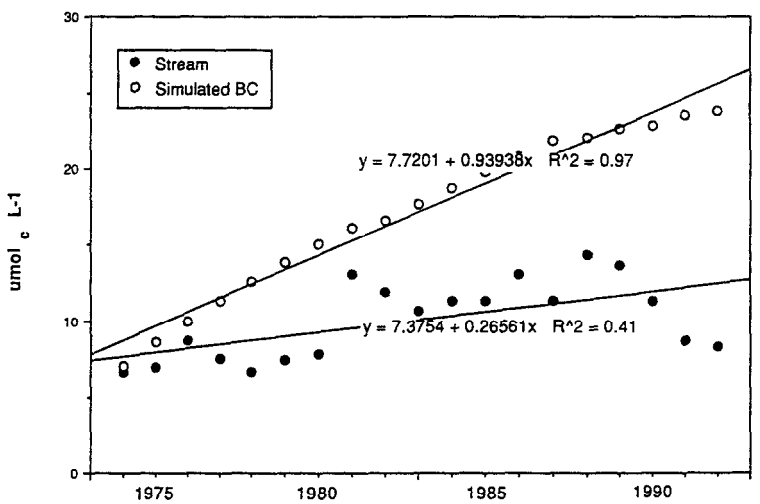

Fig. 12. Regression equations for measured streamwater SO_4^{2-} concentration on Coweeta watershed 18 from 1970 to 1990 and simulated BC horizon soil solution SO_4^{2-} concentrations for years 1 through 20 of the simulation.

the laboratory studies by Harrison et al. (1989)). The Langmuir equation in the model could be adjusted so that the two regression lines in Fig. 12 match closely; however, we chose not to do this in the absence of data to support such a change. A second possibility for the differences in the simulated and observed increases is that the balance between S mineralization and microbial transformations of sulfate to organic S forms (Swank et al. 1984) is not adequately depicted in the model. Nevertheless, it is apparent that measured stream data and model output show the same time trend with regard to increasing soil and/or ecosystem S saturation.

Many of the results of these simulations are not easily predictable with simpler models and may be worthy of field investigation. For instance, the increase Al pulsing in the A and BA horizon soil solutions in the simulations may be relevant to future developments at Coweeta, given the recent observation that base saturation is decreasing in the A and BA horizons (Knoepp & Swank in press). It should be noted that the peak soil solution Al^{3+} concentrations in the simulation remained well below known toxicity thresholds for deciduous species in this ecosystem, however. Kelly et al. (1990) found that biomass reductions in red oak (*Quercus rubra*) and sugar maple (*Acer saccharum*) did not occur until soil solution Al concentrations were well above 1500 $umol_c\ L^{-1}$, nearly an order of magnitude greater than the peak values that occurred during these simulations.

The declines in exchangeable Ca^{2+} and Mg^{2+} that occurred in these simulations were designed to match recent observations in the field and do not reflect the model's predictive capability. Knoepp & Swank (in press) found 70—80% reductions in exchangeable Ca^{2+} and Mg^{2+} from 1970 to 1990 in the A and BA horizons in a nearby deciduous forest ecosystem at Coweeta. The field data became known during the simulation exercise, and the model calibration was adjusted so that such declines would likely occur (i.e. by setting weathering to very low rates and adjusting inter-horizon uptake rates so that most Ca^{2+} and Mg^{2+} uptake occurred from the surface horizons). During this phase of the calibration, it became clear that the rate and nature of soil change are very sensitive to changes in the 'Percent uptake by horizon' menu, which allows the user to specify what percentage of each nutrient is taken up from each major soil horizon. This observation should be duly noted and accounted for by other NuCM users wishing to simulate long-term soil change.

These simulation results suggest that soil exchangeable cation pools at Coweeta change rather rapidly and that the nature of the changes are not easily predicted. The simulations suggest that exchangeable cations do not change in a unidirectional manner but undergo annual cycles (e.g. A horizon exchangeable K^+ and Mg^{2+}; Figs. 5 and 6) and multi-decade fluctuations (e.g. BC horizon exchangeable Ca^{2+} and base saturation; Figs.

4 and 7). In cases where weathering rates are relatively high (e.g. Miller et al. 1993), such short-term changes in exchangeable cations would not be expected. However, there is some support for existence of short-term changes in exchangeable cations in sites with highly-weathered soils like Coweeta. Seasonal changes in soil exchangeable cations have been observed on Walker Branch Watershed, a deciduous forest ecosystem similar to Coweeta in many ways (Johnson et al. 1988). There is also emerging evidence that soil exchangeable cations are changing much more rapidly than previously suspected in several forest ecosystems with low mineral weathering rates (Johnson et al. 1988; Binkley et al. 1989; Falkengen-Grerup et al. 1987; Knoepp & Swank in press; see also review by Johnson et al. 1991). The question raised by the NuCM model which has not yet been addressed by field sampling is that of decadal fluctuations. For example, if the simulated hypothetical ecosystem here been sampled in year 1 and in year 20 under the No Change scenario, it would have been assumed that there were no changes in base saturation (Fig. 7).

The NuCM simulations also produced the non-intuitive prediction that increased S deposition and leaching would cause increases rather than decreases in some exchangeable cations and base saturation in sub-surface horizons. There is little data to either confirm or refute this possibility at Coweeta or in similar ecosystems. However, the results of the red alder — Douglas-fir comparison by Van Miegroet & Cole (1985) suggest that such a redistribution might occur: they found reduced exchangeable base cations and base saturation in surface horizons of the red alder soil in comparison to an adjacent Douglas-fir soil, a result of high rates of nitrate leaching. In subsurface soils, however, exchangeable base cations were greater in the red alder than in the Douglas-fir soil, suggesting redistribution from surface horizons.

Conclusions

In some cases, NuCM's output followed patterns that could have been predicted with a much less complex model; for instance, the behavior of S in these soils could have been described simply with the Langmuir isotherm, with very little deviation from the NuCM's output. In other soils or with other manipulations (such as liming), pH-dependent soil SO_4^{2-} adsorption may become important, necessitating an analysis more sophisticated than that possible with the Langmuir equation alone.

In some cases, NuCM's predictions were not intuitively obvious, and suggest the need for additional field observation. For example, field sampling for temporal (both seasonal and annual) variations in exchange-

able cations could either verify or negate NuCM's predictions that changes in exchangeable cation pools are not steady and uni-directional but cyclic in nature. Manipulative studies with S inputs to test predictions of base cation redistribution would also be of considerable interest.

The NuCM model's outputs are presented not as predictions, but as illustrations of the consequences of our combined, cumulative understanding of nutrient cycling under various S deposition scenarios. The simulated effects of S deposition may have or might yet occur at Coweeta, depending upon the degree to which the model and its input parameters accurately represent the important processes governing nutrient cycling in this ecosystem.

Acknowledgements

Research supported by Cooperative Research Agreement No. 29-632 with the Southeastern Forest Experiment Station, US Forest Service. Technical advice on the NuCM model from Ron Munson is greatly appreciated.

References

Aber JD, Botkin DB & Melillo JM (1980) Predicting the effects of different harvesting regimes on productivity and yield in northern hardwoods. Can. J. For. Res. 9: 10—14

Binkley D, Valentine D, Wells C & Valentine U (1989) An empirical model of the factors contributing to 20-yr decrease in soil pH in an old-field plantation of loblolly pine. Biogeochemistry 8: 39—54

Christopherson N, Seip HM & Wright RF (1982) A model for streamwater chemistry at Birkenes, Norway. Water Resour. Res. 18: 977—996

Cole DW, Gessel SP & Dice SF (1968) Distribution and cycling of nitrogen, phosphorus, potassium, and calcium ina second-growth Douglas-fir forest. In: Young HE (Ed) Primary Production and Mineral Cycling in Natural Ecosystems (pp 197—213). University of Maine Press, Orono, Maine

Cosby BJ, Hornberger GM, Galloway JN & Wright RF (1985) Modeling the effects of acid deposition: Assessment of a lumped parameter model of soil water and streamwater chemistry. Water Resour. Res. 21: 51—63

Curlin JW (1970) Nutrient cycling as a factor in site productivity and forest fertilization. In: Youngberg CT & Davey CR (Eds) Tree Growth and Forest Soils (pp 313—326). Oregon State University Press, Corvallis

Duvigneaud P & Denaeyer-DeSmet P (1970) Biological cycling of minerals in temperate deciduous forests. In: Reichle DE (Ed) Analysis of Forest Ecosystems (pp 199—255). Springer-Verlag, New York

Falkengren-Grerup U, Linnermark N & Tyler G (1987) Changes in acidity and cation pools of south Swedish soils. Chemosphere 16: 10—12

Goldstein RA, Gherini SA, Chen CW, Mok L & Hudson RJM (1984) Integrated acidification study (ILWAS): A mechanistic ecosystem analysis. Phil. Trans. R. Soc. Lond. B 305: 259—279

Harrison RB, Johnson DW & Todd DE (1989) Sulfate adsorption and desorption in a variety of forest soils. J. Environ. Qual. 18: 419—426

Johnson DW, Cresser MS, Nilsson SI, Turner Julrich B, Binkley D & Cole DW (1991) Soil changes in forest ecosystems: Evidence for and probable causes. Proc., Royal Society of Edinburgh 97B: 81—116

Johnson DW, Henderson GS & Todd DE (1988) Changes in nutrient distribution in forests and soils of Walker Branch Watershed over an eleven-year period. Biogeochemistry 5: 275—293

Johnson DW & Lindberg SE (Eds) (1991) Atmospheric Deposition and Forest Nutrient Cycling: A Synthesis of the Integrated Forest Study. Ecological Series 91, Springer-Verlag, New York, 707 pp

Johnson DW & Reuss JO (1984) Soil mediated effects of atmospherically-deposited sulphur and nitrogen. Phil. Trans. Roy. Soc. Lond. B 305: 383—392

Kelly JM, Schaedle M, Thornton FC & Joslin JD (1990) Sensitivity of tree seedlings to aluminum: II. Red oak, sugar maple, and European beech. J. Environ. Qual. 19: 172—179

Kimmins JP, Scoullar KA, Feller MC, Chatarpaul L & Tsze KM (1984) Simulation of potential long-term effects of intensive forest management using FORCYTE-10. In: New forest for a changing world. Proceedings of the 1983 Convention of the Society of American Foresters, Portland, Oregon October 16—20, 1983

Knoepp JD & Swank WT (1994) Long-term soil chemistry changes in aggrading forest ecosystems. Soil Sci. Soc. Amer. J. (in press)

Liu S, Munson R, Johnson DW, Gherini S, Summers K, Hudson R, Wilkinson K & Pitelka LF (1991a) The Nutrient Cycling Model (NuCM): Overview and application. In: Johnson DW & Lindberg SE (Eds) Atmospheric Deposition and Forest Nutrient Cycling: A Synthesis of the Integrated Forest Study (pp 583—609). Ecological Series 91, Springer-Verlag, New York, 707 pp

Liu S, Munson R, Johnson DW, Gherini S, Summers K, Hudson R, Wilkinson K & Pitelka LF (1991b) Application of a nutrient cycling model (NuCM) to northern mixed hardwood and southern coniferous forests. Tree Physiology 9: 173—182

Miller EK, Blum JD & Friedland AJ (1993) Determination of soil exchangeable-cation loss and weathering rates using Sr isotopes. Nature 362: 438—441

Miller HG, Cooper JM, Miller JD & Pauline OJL (1979) Nutrient cycles in pine and their adaption to poor soils. Can. J. For. Res. 9: 19—26

Munsen RK, Liu S, Gherini SA, Johnson DW, Wilkinson KJ, Hudson RJM, White KS & Summers KV (1992) NuCM Code Version 2.0: An IBM POC Code for Simulating Nutrient Cycling in Forest Ecosystems. Tetra-Tech, Inc. Hadley, MA

Pastor J, Gardner RH, Dale VH & Post WM (1987) Successional changes in nitrogen availability as a potential factor contributing to spruce decline in boreal North America. Can J. For. Res. 17: 1394—1400

Rennie PJ (1955) The uptake of nutrients by mature forest growth. Plant Soil 7: 49—95

Reuss JO & Johnson DW (1986) Acid Deposition and the Acidification of Soil and Water. Ecological Studies No. 59. Springer-Verlag, New York, 118 pp

Richter DD, Johnson DW & Dai KH (1991) Cation exchange reactions in acid forested soils: Effects of atmospheric pollutant deposition. In: Johnson DW & Lindberg SE (Eds) Atmospheric Deposition and Forest Nutrient Cycling: A Synthesis of the Integrated Forest Study (pp 341—357). Ecological Series 91, Springer-Verlag, New York, 707 pp

Shugart HH, Reichle DE, Edwards NT, Kercher JR (1976) A model of calcium-cycling in an east Tennessee Liriodendron forest: Model structure, parameters, and analysis in the frequency domain. Ecology 57: 99—109

Sollins P, Grier Cc, McCorison FM, Cromack K, Fogel R & Fredriksen RL (1980) The internal element cycles of an old-growth Douglas-fir ecosystem in western Oregon. Ecol. Monogr. 50: 261—285

Sposito G (1977) The Gapon and Vaneslow selectivity coefficients. Soil Sci. Soc. Amer. J. 48: 531—536

Swank WT, Fitzgerald JW & Ash JT (1984) Microbial transformation of sulfate in forest soils. Science 223: 182—184

Swank WT, Reynolds LJ & Vose JM (1991) Appendix tables ch1, 2, and 3. In: Johnson DW & Lindberg SE (Eds) Atmospheric Deposition and Forest Nutrient Cycling: A Synthesis of the Integrated Forest Study (pp 612, 634, and 656). Ecological Series 91, Springer-Verlag, New York, 707 pp

Swank WT & Waide JB (1988) Characterization of baseline precipitation and stream chemistry and nutrient budgets for control watersheds. In: Swank WT & Corssley DA (Eds) Forest Hydrology and Ecology of Coweeta (pp 57—79). Springer-Verlag, New York

Swank WT, Reynolds LJ & Vose JM (1991) Appendix data. In: Johnson DW & Lindberg SE (Eds) Atmospheric Deposition and Forest Nutrient Cycling: A Synthesis of the Integrated Forest Study (pp 583—609). Ecological Series 91, Springer-Verlag, New York, 707 pp

Van Miegroet H & Cole DW (1985) Acidification sources in red alder and Douglas-fir soils — Importance of nitrification. Soil Sci. Soc. of Amer. J. 9: 1274—1279